Advanced Steel Construction – Vol. 15 No. 3 (2019) 288–296
DOI:10.18057/IJASC.2019.15.3.9

EXPERIMENTAL STUDY OF THE BEARING CAPACITY OF LONG-SPAN PROFILED STEEL SHEET–CONCRETE COMPOSITE SLABS

Xiao-Xiang He [1, 2] , Guo-Chang Li [2, *] and Zhi-Jian Yang [2]

[1] *School of Civil Engineering, Dalian University of Technology, Dalian, China*
[2] *School of Civil Engineering, Shenyang Jianzhu University, Shenyang, China*
** (Corresponding author: E-mail: liguochang0604@sina.com)*

ABSTRACT

This paper presents an experimental study on the structural performance of 26 composite slab specimens having trapezoidal and dovetail profiles. The influence of the span, details of the end anchorage, and cross-sectional depth on the mechanical performance and failure modes of the specimens was discussed. The effects of the thickness of the profiled steel sheets and additional reinforcement of the bottom on the longitudinal shear bearing capacity of long-span dovetail-profiled composite slabs were also investigated. Research on long-span composite slabs accounting for different details of the end anchorage and steel profiles is limited in the literature. The test results indicated that the end anchorage can significantly improve the mechanical performance and ultimate bearing capacity of composite slabs, whereas additional reinforcement and thick profiled steel sheets can slightly increase their bearing capacity. The test results also showed that, in long-span flooring systems, dovetail-profiled composite slabs have a higher load bearing capacity than trapezoidal-profiled composite slabs.

ARTICLE HISTORY

Received: 6 March 2019
Revised: 3 April 2019
Accepted: 7 April 2019

KEYWORDS

Long-span composite slabs;
Experimental study;
Load bearing capacity;
Failure mode;
Longitudinal shear

Copyright © 2019 by The Hong Kong Institute of Steel Construction. All rights reserved.

1. Introduction

Profiled steel sheet–concrete composite slabs are widely used in steel structures and steel–concrete composite structures owing to their advantages of rapid construction, enhanced safety, and high cost efficiency. During the design and construction of composite slab floors, a profiled steel sheet serves both as a template during construction and as load-bearing reinforcement during the service life of the slabs [1–3]. Although the performance of a composite slab is affected by the inherent material properties, geometrical characteristics, boundary conditions, and mode of external loading, it is mainly governed by the interactions at the profiled steel sheet–concrete interface. Profiled steel sheet–concrete composite slabs subjected to external loading, primarily experienced longitudinal shear or flexural failure [4–8]. For composite slabs with end anchorage such as a welded stud, the slip at the profiled steel sheet–concrete interface can be reduced, whereas the bond between the steel sheet and concrete can be enhanced. Consequently, their strength and rigidity can be improved [9–12].

Generally, the span of simply supported composite slabs is less than 4.5 m and that of continuous composite slabs is less than 5.1 m [13]. Composite slabs with short spans can enable rapid construction, and thus, have high operating efficiencies despite their inherent disadvantages. As a long-span structure is constructed by composite slab of short span, numerous filler beams and connectors welding with a high workload are required. Long-span composite slabs require several temporary supports but few filler beams. As the additional costs of the temporary supports are smaller than the use of filler beams, long-span composite slabs are significantly more cost efficient than short-span ones [14].

Extensive studies on the behavior of composite slabs have been reported in the literature. Porter and Greimann [1], Jolly and Lawson [15] investigated the effect of end-anchorage stud on the behavior of composite slabs by test. They found that the composite slabs without end anchorage experienced longitudinal shear failure at the steel sheet–concrete interface, whereas those with end anchorage underwent failure through local buckling or tearing of the steel sheet near the studs. Furthermore, the end anchorage contributed to a significant improvement in the shear bond strength, bearing capacity, and ductility of the composite slabs. Chen [16] conducted an experimental study on the behavior of simply supported and continuous composite slabs and found that the longitudinal shear strength was governed by the bond slip at the profiled steel sheet–concrete interface and not by the anchoring strength of the studs. Moreover, the longitudinal shear strength obtained from the linear regression of the test results of the simply supported composite slabs with end anchorage could be used to compute the bearing capacity of continuous composite slabs. Valivonis [7] distinguished three stages in the failure of the steel sheet–concrete interface of composite slabs: elastic deformation, plastic deformation, and cracking and failure. He found that the shear strength at the steel sheet–concrete interface was significantly affected by the cross-sectional shape of the profiled steel sheet, transverse pre-compressing force, and restraining capacity of the interface. Chen et al. [5] studied the shear-bond failure mechanism and behavior of composite slabs and suggested that the distribution of the longitudinal shear stress along the length of the composite slabs was nonuniform. Moreover, the shear strength of the composite slabs was mainly governed by the same property of the shear span. Based on an investigation of the effect of end-anchorage studs on the longitudinal shear strength of composite slabs, Chen et al. [9] suggested that the contribution of the studs to the longitudinal shear bearing capacity of the composite slab was not simply an addition of the shear strengths of the individual studs.

Studies have also been conducted on composite slabs having different cross-sectional geometries. In a study on composite slabs decked with profiled steel sheets having three different cross-sectional geometries and subjected to static and dynamic loads, Bode and Minas [17] found that all the different composite slabs having an end anchorage exhibited a high load bearing capacity and ductility. Gholamhoseini et al. [18] conducted an experimental study on eight full-scale simply supported composite slab specimens using four types of profiled deckings subjected to a four-point bending to identify the influence of the type of decking on the shear–slip relationship. The experimental results revealed that all the four types of specimens underwent longitudinal shear failures, whose strength decreased with the increase in the shear span.

Regarding composite slabs with additional longitudinal reinforcements, Johnson and Shepherd [19] found that the additional reinforcement placed above the troughs of the steel sheet, significantly affected the shear strength. The failure of composite slabs is typically governed by deflection, and it may not be possible to completely utilize the advantage of the additional reinforcements.

Bending tests of full-scale composite slabs typically follow the standard experimental methods provided in Eurocode 4[3] or BS 5950-4 [20]. Ríos et al. [21] compared the four and six-point loading methods using numerical analysis and found that the former was suitable for concentrated loads, whereas the latter was appropriate for uniform loads. Abdullah and Easterling [22] simulated a test of full-scale composite slab specimens using a new elemental test for cost efficiency and demonstrated that the elemental test results agreed well with the test results of the full-scale specimens.

The performance of long-span composite slabs has also been studied. Widjaja and Easterling [14] found that their performance was generally governed by deflection. In an experimental study on long-span composite slabs decked with profiled steel sheets with depths of not less than 200 mm, Brekelmans et al. [23] found that the fundamental theory provided in Eurocode 4: Part 1.1 was also applicable to long-span composite slabs.

The above-mentioned literature review reveals that previous research generally focused on composite slabs with short spans from 1.2m to 4.5m, and research on long-span composite slabs is limited. This paper presents an experimental study on the performance and failure behavior of composite

slabs with different spans. A total of 26 profiled steel-sheet–concrete composite slab specimens having two different cross-sectional geometries were tested. Parameters such as the cross-sectional geometry of the profiled steel sheet, depth of the composite slab, anchoring stud configuration, and additional reinforcement were investigated with the aim of providing test data and theoretical input for the design and application of long-span composite slabs.

2. Set-up of Experimental Test

2.1. Design of test specimens

A total of 26 simply supported composite slab specimens were designed, among which 11 were decked with trapezoidal-shaped profiled steel sheet and 15 were decked with dovetail-shaped profiled steel sheet.

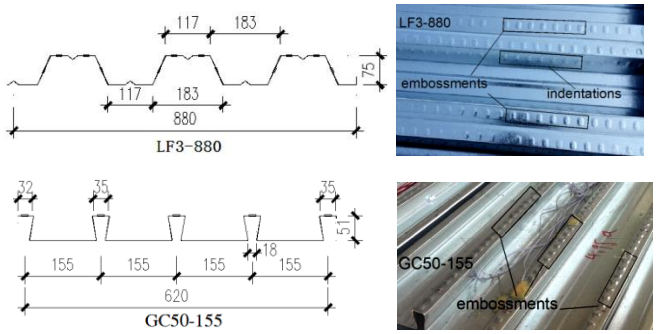

(a) Cross-section of the steel sheets (b) Details of surface features

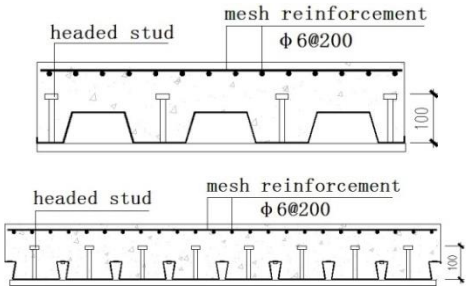

（c）End anchorage details of the

Fig. 1 Details of test specimens

Table 1
Details of test specimens with the LF3-880 type steel sheet

No.	Specimens	Span L(mm)	Slab depth d(mm)	Sheeting thickness t(mm)	Span/depth (mm)	End anchorage	Additional reinforcement
1	OBI-1	2000	180	1.0	11.1	D19	No
2	OBI-2	2000	180	1.0	11.1	D19	No
3	OBI-3	2000	180	1.0	11.1	No	No
4	OBII-1	3400	150	1.0	22.7	D19	No
5	OBII-2	3400	150	1.0	22.7	D19	No
6	OBIII-1	4800	160	1.0	30	No	No
7	OBIII-2	4800	160	1.0	30	D19	No
8	OBIII-3	4800	200	1.0	24	D19	No
9	OBIV-1	6000	200	1.0	30	D19	4φ10
10	OBIV-2	6000	200	1.0	30	No	4φ10
11	OBIV-3	6000	250	1.0	24	D19	4φ10

The following parameters were investigated:
(1) Cross-sectional geometry of the profiled steel sheets: trapezoidal profile LF3-880 and dovetail profile GC50-155,
(2) Span and depth of the composite slab,
(3) Configuration of the end-anchorage studs,
(4) Additional reinforcement (one for each trough of the profiled steel sheet for specimens with a span of 6.0 m).

Table 2
Details of test specimens with the GC50-155 type steel sheet

No.	Specimens	Span L(mm)	Slab depth d(mm)	Sheeting thickness t(mm)	Span/depth (mm)	End anchorage	Additional reinforcement
1	NBI-1	2000	180	1.0	11.1	No	No
2	NBI-2	2000	180	1.0	11.1	D19	No
3	NBI-3	2000	180	1.0	11.1	D19	No
4	NBII-1	3400	150	1.0	22.7	D19	No
5	NBII-2	3400	150	1.0	22.7	D19	No
6	NBIII-1	4800	200	1.0	24	D19	No
7	NBIII-2	4800	160	1.2	30	D19	No
8	NBIII-3	4800	160	1.0	30	D19	No
9	NBIII-4	4800	160	1.0	30	No	No
10	NBIV-1	6000	250	1.0	24	D19	No
11	NBIV-2	6000	200	1.2	30	D19	No
12	NBIV-3	6000	200	1.0	30	D19	No
13	NBIV-4	6000	200	1.0	30	No	No
14	NBIV-5	6000	200	1.2	30	D19	8φ10
15	NBIV-6	6000	200	1.0	30	D19	8φ10

Table 3
Geometry and strength properties of steel sheets

Types	Thickness t（mm）	Area A_p （cm²/m）	I_x(cm⁴/m)	f_p(N/mm²)	f_u (N/mm²)
LF3W-880	1.0	14.7	156.68	335	566
GC50-155	1.0	19.3	75.60	330	461
GC50-155	1.2	22.0	85.60	414	512

Tables 1 and 2 list the parameters of the specimens. The depth design of the specimens accounted for the deflection and longitudinal shear strength required by the composite slabs. The specimens were designed with depth-to-span ratios of not less than 1/30 [24]. The trapezoidal-profiled steel sheets had embossments on the upper flange surface and indentations on the web surface, and the dovetail-profiled steel sheet had embossments on the upper flange surface. Fig. 1(a) and Fig. 1(b) show the cross-sectional geometries and surfaces of both the profiled steel sheets. Table 3 lists the material properties of both the profiled steel sheets. The additional reinforcement has a tensile strength of 540 N/mm^2 and yield strength of 360 N/mm^2. The end anchorage stud has a diameter of 19 mm and length of 100 mm. It is penetration-welded at the trough of the profiled steel sheets and welded to the steel sheet of the support. Four and eight studs were welded at the anchoring ends of the trapezoidal and dovetail-profiled steel sheets, respectively. The width of the trapezoidal-profiled composite slab specimens is 880 mm. The dovetail-profiled specimens used two profiled steel sheets joined transversely and with a width of 1240 mm, as shown in Fig. 1(c). To avoid cracking induced by concrete-contraction, φ6@200 reinforcement steel meshes were arranged at the compressive zone of the specimens. The cubic compressive strength of concrete is 33.1 N/mm^2.

2.2. Experimental scheme and layout of measurement points

Different loading devices were used according to the different spans of the specimens. A four-point loading device was used for specimens with a span smaller than 2.0m, with two equal point loads applied by a load-distribution beam, as illustrated in Fig. 2(a). A six-point loading device was used for the specimens with spans of 3.4m, 4.8m, and 6.0 m, with four equal point loads applied by two levels of load-distribution beams, as displayed in Fig. 2(b).

The vertical load was applied with a staged increase, which was about 10% of predicted bending moment capacity of the specimen. At each load level, the vertical load held for 5 minutes to observe and record the testing phenomenon.

When the test load reduced to below 80% of the ultimate load, and the mid-span deflection was more than 1/50 of the span, the test was terminated.

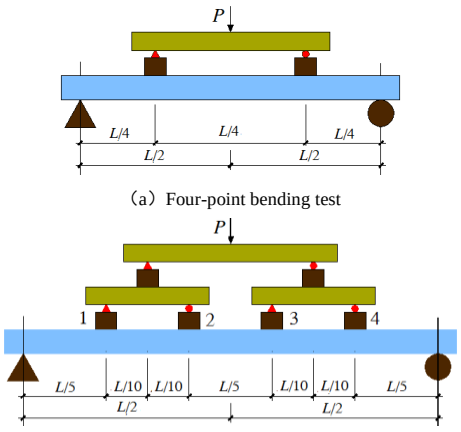

Fig. 2 Schematic view of the experimental setup

The external load was measured using load sensors placed in front of the jacks. The strains of profiled steel sheet and concrete were measured using strain gauges. The displacement and slip at the steel sheet–concrete interface were measured using linear variable differential transformer (LVDT) sensors. Fig. 3 shows the configuration of the LVDT sensors.

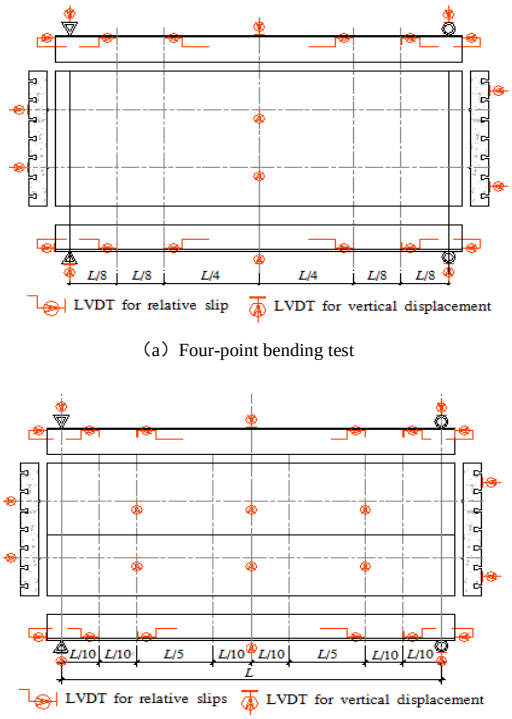

Fig. 3 Arrangement of the LVTDs

3. Test Procedures and Failure Modes

For a clear presentation of the tests, the specimens with spans of 2.0 and 3.4 m are referred to as short-span specimens, whereas those with spans of 4.8 and 6.0 m are referred to as long-span specimens.

3.1. Composite slab specimens without end anchorage

In this study, six specimens without an end anchorage were tested: three had trapezoidal profiles with different spans, and another three had dovetail profiles with different spans.

3.1.1. Trapezoidal-profiled specimens

The load bearing capacity of the trapezoidal-profile specimens decreased abruptly after reaching the ultimate load. At this point, the outer edges of the steel sheet and concrete at the mid-span developed large longitudinal cracks (Fig. 4(a)), the specimens exhibited significant slip at the anchoring end (Fig. 4(b)), and there were shear cracks running through the length of the specimens. Moreover, the upper and bottom flanges and troughs of the profiled steel sheet at the mid-span underwent significant buckling (Fig. 4c), leading finally to brittle longitudinal shear failures.

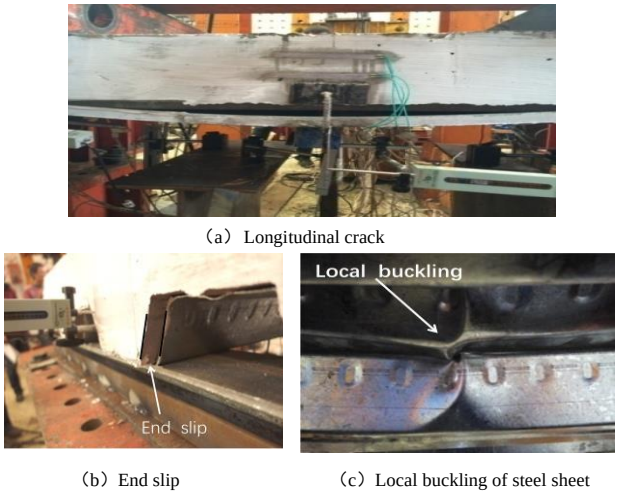

(a) Longitudinal crack

(b) End slip (c) Local buckling of steel sheet

Fig. 4 Failure mode of OBI-3

Two long-span specimens, OBIII-1 and OBIV-2, had the same shear span-depth ratio and were loaded similarly. The long-span specimens exhibited similar behavior to those of the short-span ones during the initial stage of the loading but developed longitudinal cracks and end-slip at a load of approximately 0.45 P_u. After the onset of slipping, the load increased slowly, whereas the mid-span deflection increased more rapidly, resulting in longitudinal shear failure. At the point of failure, the bond between the steel sheet and concrete interface at the mid-span of the specimens failed (Fig. 5(a)) and the supporting ends of the specimens exhibited significant slip (Fig. 5(b)). In addition, the troughs of the steel sheet appeared local buckling near mid-span loading point 4 (Fig. 5(c)).

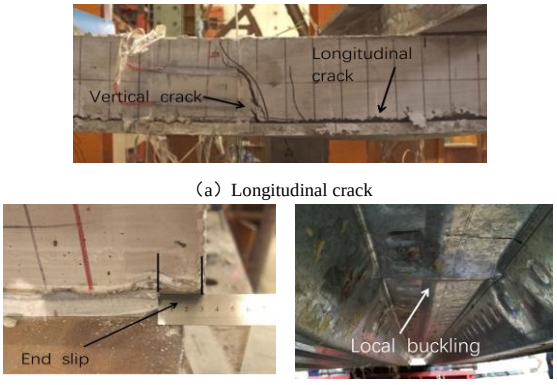

(a) Longitudinal crack

(b) End slip (c) Local buckling of steel sheet

Fig. 5 Failure mode of OBIII-1 and OBIV-2

3.1.2. Dovetail-profiled specimens

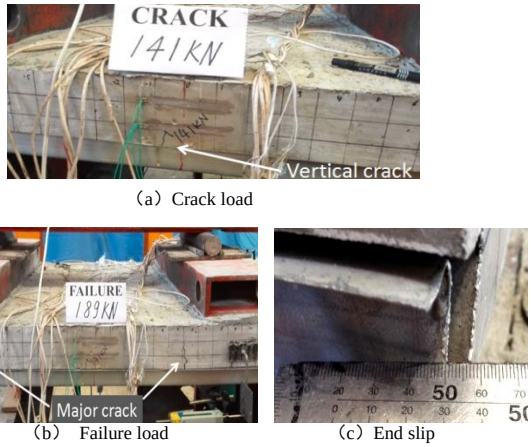

(a) Crack load

(b) Failure load (c) End slip

Fig. 6 Failure behaviors of NBI-1

At a load of approximately 98 kN (0.52 P_u), NBI-1, a short-span specimen, exhibited an abrupt increase in the mid-span deflection and bond slip at the steel-sheet – concrete interface. At a load of 141 kN (0.75 P_u), the specimen developed vertical cracks at the mid-span (Fig. 6(a)). At a load of 189 kN (P_u), the major cracks near the mid-span loading points became wider (Fig. 6(b)) and the edges of the steel sheet at the two sides of the specimen separated from the concrete and bloated outward. In addition, the mid-span deflection increased rapidly, the bond at the profiled steel-sheet–concrete interface started slipping at the ends of the specimen (Fig. 6(c)), and the test load rapidly decreased, resulting in a longitudinal shear failure.

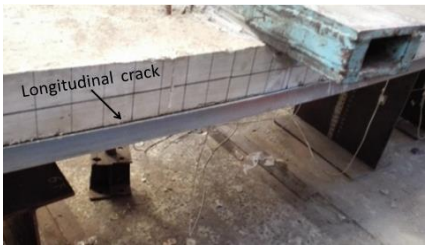

（a） Longitudinal crack

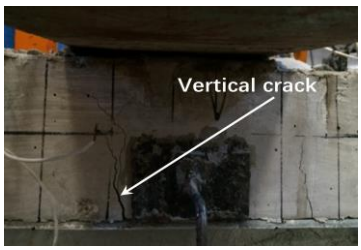

（b）Vertical cracks

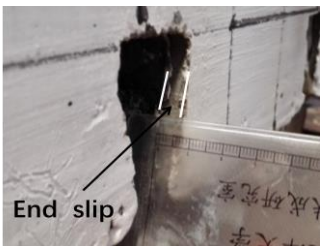

（c）End slip

Fig. 7 Failure mode of NBIII-4

Long-span specimens NBIII-4 and NBIV-4 exhibited similar behavior during the initial stage of loading. At a load of approximately 0.4 P_u, the specimens exhibited slipping at the steel sheet – concrete interface and longitudinal cracks at both sides of mid-span loading points 2 and 3 (Fig. 2(b)). At a load of approximately 0.65 P_u, the specimens exhibited vertical cracks at the mid-span side of loading point 3. At a load of approximately 0.8 P_u, the steel sheet at the two sides of the specimens exhibited longitudinal cracks and bloated outward near loading points 1 and 4 (Fig. 7(a)), which was accompanied by a temporary load decrease. As the load stabilized, the load bearing capacity of the specimens increased continuously. At the ultimate load, P_u, the width of the vertical cracks rapidly increased (Fig. 7(b)), and the specimens experienced rapid slipping at the steel-sheet–concrete interface (Fig. 7(c)), resulting in a longitudinal shear failure.

3.2. Composite slab specimens with end –anchorage studs

3.2.1. Trapezoidal-profiled specimens

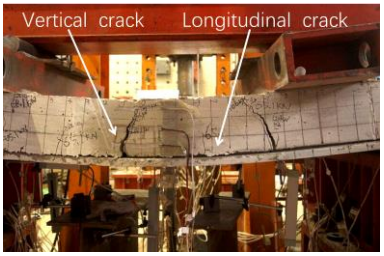

(a) Longitudinal and vertical crack

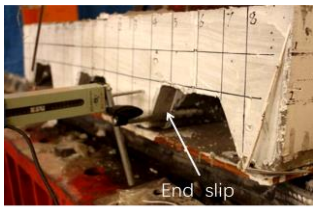

(b) End slip

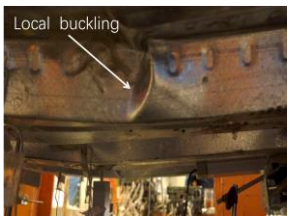

（c）Local buckling of the steel sheet

Fig. 8 Failure mode of short-span trapezoidal-profile specimen

Short-span specimens OBI-1 and OBI-2 exhibited the following behavior during the loading: At a load of approximately 0.3 P_u, the first vertical crack developed in the concrete near the loading point. At a load of approximately 0.5 P_u, the specimens exhibited slight slipping at the ends and longitudinal cracks in the steel sheet–concrete interface near the loading points. As the test load increased, the longitudinal cracks extended to the ends of the specimens. At the ultimate load, P_u, the mid-span deflection rapidly increased, the bond between the steel sheet and concrete at the two sides failed (Fig. 8(a)), and tearing finally occurred in the steel sheet around the studs. The slipping at the end of the specimens rapidly increased (Fig.8(b)), local buckling deformation developed in the steel sheet below the loading point (Fig. 8(c)), and the specimens lost their bearing capacity, resulting in longitudinal shear failures.

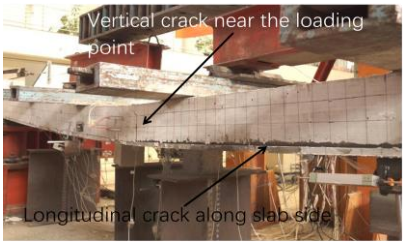

（a）Longitudinal crack

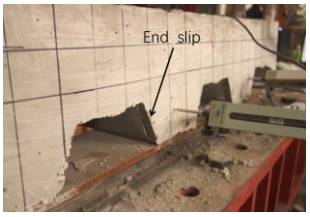

(b) End slip

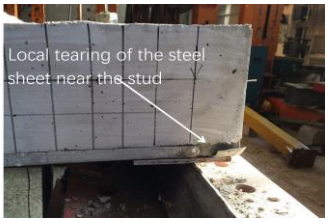

（c）Local tearing of the steel sheet

Fig. 9 Failure mode of long-span trapezoidal-profile specimen

At a load of approximately 0.2 P_u, the long-span composite slab specimens having anchoring studs developed vertical cracks near mid-span loading point 3. At a load of approximately 0.3 P_u, first, longitudinal cracks developed near mid-span loading points 2 and 3, and as the load increased, they extended toward the supports. Moreover, the specimens underwent slipping at the steel sheet–concrete interface. During the latter stage of loading, the mid-span deflection increased more rapidly, the longitudinal cracks at the steel-sheet–concrete interface extended to the ends of the specimens, and the specimens lost their bearing capacity, resulting in longitudinal shear failures. At the point of failure, the bond of the steel sheet–concrete interface at the mid-span failed (Fig. 9(a)), the slipping at the ends of the specimens became significant (Fig. 9(b)), and the profiled steel sheet experienced local tearing at the ends, but no buckling (Fig. 9(c)).

3.2.2. Dovetail-profiled specimens

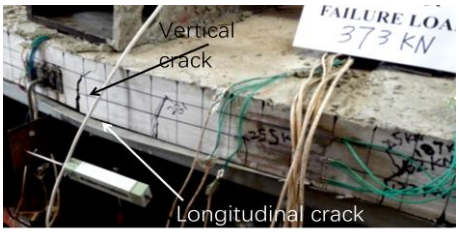

（a） Longitudinal crack

（b） End slip

（c） Local tearing of the steel sheet

Fig. 10 Failure mode of short-span dovetail-profile specimen

At a load of 130 kN (0.35 P_u), NBI-3, a short-span specimen, developed vertical cracks near the loading points. As the load increased, longitudinal cracks developed at the steel sheet–concrete interface at the two sides of the specimen at the mid-span. At a load of 240 kN (0.64 P_u), significant slipping developed at the steel sheet–concrete interface at the ends of the specimen. As the load increased, the steel sheet at the two sides at the mid-span bloated outward (Fig. 10(a)), and the mid-span deflection increased rapidly. At a load of 373 kN (P_u), tearing developed in the troughs of the steel sheet at the ends of the specimen (Fig. 10(b) and Fig. 10(c)), the slipping rapidly increased, and the specimen was no longer appropriate for load bearing, resulting in a longitudinal shear failure.

（a）Longitudinal crack

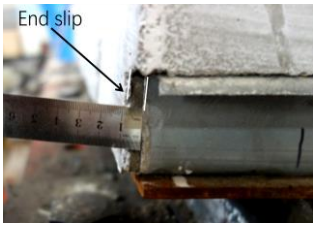

（b）End slip

（c）Crack of concrete beneath loading point

Fig. 11 Failure mode of long-span dovetail-profile specimen

The failure behavior of the long-span specimens was described using the most typical specimen, NBII-2. At a load of 76 kN (0.48 P_u), vertical cracks developed at the mid-span and longitudinal cracks developed at the steel sheet–concrete interface at the two sides of the specimen in the regions of mid-span loading points 3 and 4. Moreover, as the load increased, the cracks extended toward the supports. At a load of 128 kN (0.82 P_u), the specimen underwent significant slipping at the steel sheet–concrete interface (Fig.s 11(b)). As the load continued to increase, the steel sheet at the two sides of the specimen bloated outward, the width of the major cracks near loading point 3 increased, the mid-span deflection exceeded L/50, and the ultimate load, P_u, was 157 kN. The other long-span specimens exhibited failure behavior similar to that of specimen NBII-2.

The cracking load P_{cr}, slipping load P_s, and ultimate load P_u of dovetail-profiled composite slab specimens increase with the increasing of thickness of steel sheets, depths of cross-sectional, and arrangement of additional reinforcement.

4. Test Results and Discussion

A comparative analysis of the different specimens based on the depth of slabs was conducted to study the performance and failure behavior of the short and long-span specimens.

4.1. Trapezoidal-profiled specimens

4.1.1. Short-span specimens

Fig. 12 shows the load–mid-span deflection curves and load–end slip curves of the specimens with a span of 2.0 m. Fig. 12(a) shows that during the initial stage of loading, the specimens have similar stiffness and behavior. Furthermore, the bearing capacity of the specimens with an end anchorage (OBI-1 and OBI-2) is higher than that of those without it (OBI-3) by 174% and 129%, respectively. Fig. 12(b) shows that as the load increases, the bond at the steel sheet–concrete interface of the specimens without an end anchorage fails after the onset of slipping. In addition, the load bearing capacity significantly decreases, the slipping continues to increase, and the specimens are no longer suitable for load bearing and fail. Contrastingly, the specimens with an end anchorage have a higher bearing capacity because the anchoring studs serve to restrain the slipping and increase the interaction at the profiled steel sheet–concrete interface. The composite slab specimens without an end anchorage exhibit more evident longitudinal shear failures than those with it. Contrastingly, the latter exhibit an extremely good ductility and a significantly higher bearing capacity than the former specimens.

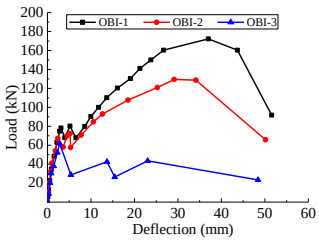

（a）Load- mid-span deflection curves

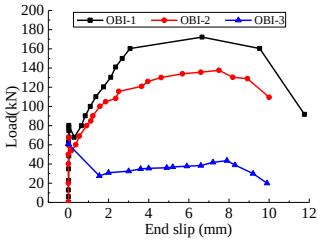

（b）Load - end slip curves

Fig. 12 Load–deflection and Load–slip curves of the specimens with a span of 2.0 m

4.1.2. Long-span specimens

All the thin slab specimens with a span of 3.4 m had an end anchorage and exhibited the same failure behavior. Compared with thick slab specimens with a span of 2.0 m having a similar end anchorage, they experienced similar longitudinal shear failures, but had a good loading bearing capacity and much better ductility, as shown in Fig. 13(a) and Fig. 13(b).Please, do not alter the title page header and make sure that you comply with the headers of the other pages.

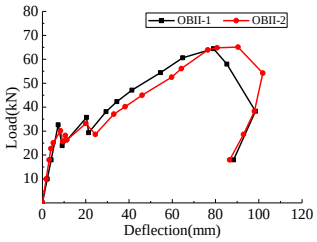

（a）Load – mid-span deflection curves

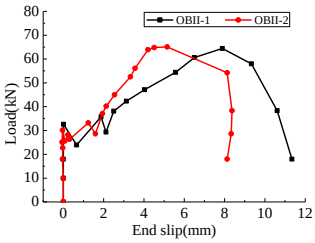

（b）Load - end slip curves

Fig. 13 Load–deflection and Load–slip curves of the specimens with a span of 3.4 m

At spans of 4.8 m and 6.0 m, all the specimens without an end anchorage and those with it exhibited similar failure behavior within their separate groups, but with the two groups of specimens displaying different failure behavior compared to each other.

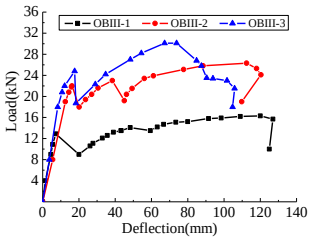

（a）Load – mid-span deflection curves

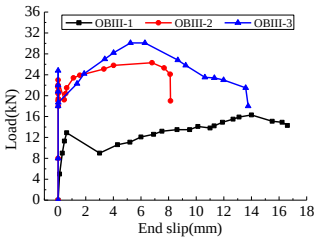

（b）Load - end slip curves

Fig. 14 Load–deflection and Load–slip curves of the specimens with a span of 4.8 m

The load - mid-span deflection curves shown in Fig. 14(a) and Fig. 15(a) and the load - end slip curves shown in Fig. 14(b) and Fig. 15(b) reveal that the specimens with and without an end anchorage exhibit similar behavior during the initial stage of the loading. However, as the bond at the steel sheet–concrete interface fails, the specimens without an end anchorage experience longitudinal shear failure owing to the large end slip. Contrastingly, the specimens with an end anchorage have a significantly high bearing capacity and ductility and undergo ductile longitudinal shear failure because the studs serve to retrain the slip at the profiled steel sheet–concrete interface and the end slip is affected by the external loading. At a span of 4.8 m, the specimen with an end anchorage, OBIII-2, has a higher bearing capacity than the specimen without it, OBIII-1, by 41.7%. At a span of 6.0 m, the specimen with an end anchorage, OBIV-2, has a higher bearing capacity than the specimen without it, OBIV-1, by 31.3%. The high-depth specimens possess significantly strong cross-sectional flexural stiffness and longitudinal shear strengths. More specifically, at a span of 4.8 m, specimen OBIII-3 has a higher bearing capacity than specimen OBIII-2 by 32%. Furthermore, at span of 6.0 m, specimen OBIV-3 has a higher bearing capacity than OBIV-2 by 16.4%.

Table 4
Test result for load carrying capacity and failure mode of trapezoidal-profile specimens

No	Specimens	P_{cr}（kN）	P_s（kN）	$P_{1/250}$（kN）	P_u（kN）	M_u (kN.m)	M_p (kN.m)	M_u/M_p	Δ_u (mm)	s (mm)	Failure mode
1	OBI-1	50.0	74.8	84.6	171.8	44.3	52.8	0.84	32.2	3.6	ductile
2	OBI-2	41.2	62.1	72.5	142.5	36.9	52.8	0.7	31.62	7.5	ductile
3	OBI-3	38.3	57.5	30.6	62.2	16.9	52.8	0.32	3.52	12	brittle
4	OBII-1	14	17.1	19.1	56.4	31.7	40.4	0.78	75.60	7.5	ductile
5	OBII-2	13	19	17.6	56.1	31.5	40.4	0.78	77.1	7.6	ductile
6	OBIII-1	12	15	9.5	16.3	18.0	44.5	0.4	119.0	14.0	brittle
7	OBIII-2	9	18	13.2	23.1	22.9	44.5	0.51	103.6	7.2	ductile
8	OBIII-3	10	22	16.5	30.5	30.1	61.1	0.49	66.79	6.9	ductile
9	OBIV-1	12	27.5	21.9	35.2	44.3	74.7	0.59	100.5	6.8	ductile
10	OBIV-2	11	19.5	19.5	26.8	36.7	74.7	0.49	145.2	17.6	brittle
11	OBIV-3	15	19	27.6	41	53.6	100.7	0.53	70.62	6.3	ductile

Note：P_{cr} is the cracking load of concrete; P_s is the slipping load; $P_{1/250}$ is the load about mid-span deflection reaches 1/250 span; P_u is the ultimate load; M_u is the test ultimate moment; M_p is the plastic moment; Δ_u is the mid-span deflection corresponding to the ultimate load; s is the end slip corresponding to the ultimate load

Table 4 lists the characteristic loads, failure behavior, measured bearing capacity, and theoretical plastic bearing capacity of the trapezoidal-profiled specimens. Table 4 shows that the specimens with an end anchorage have a remarkably larger M_u/M_p ratio than those without it. The increase in the ratio is more at short spans than that at long spans. The increase in the ratio of the long-span specimens indicates that they have a larger bonding interface between the profiled steel sheet and concrete and a higher capacity to resist the slip at the interface. These characteristics indirectly improve the bonding at the profiled steel-sheet–concrete interface.

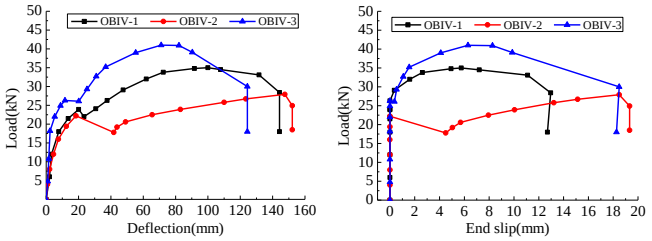

（a）Load – mid-span deflection curves （b）Load - end slip curves

Fig. 15 Load–deflection and Load–slip curves of the specimens with a span of 6.0 m

4.2. Dovetail-profiled specimens

4.2.1. Short-span specimens

Fig. 16 shows the load–deflection curves and load–slip curves of 2.0-m span dovetail-profiled specimens. It suggests that during the initial loading stage, the specimens exhibit similar behavior. As the load increases and the bond at the profiled steel sheet–concrete interface gradually fails, the specimens without an end anchorage undergo slipping at the interface and an abrupt decrease in the bearing capacity. However, owing to the better interaction between the dovetail-profiled steel sheet and concrete, which serves to better restrain the slip at the profiled steel sheet–concrete interface, the bearing capacity can be recovered. The specimens without an end anchorage experience longitudinal shear failure only after the interaction at the profiled steel sheet–concrete interface is insufficient to resist the longitudinal shear stress at the interface. The specimens with an end anchorage have a significantly better bearing capacity than those without because the studs serve to restrain the slip at the profiled steel sheet–concrete interface, thereby improving the interaction between the profiled steel sheet and concrete. All the specimens with and without the end-anchorage studs undergo evident ductile longitudinal shear failure. The bearing capacity of the specimens with an end anchorage (NBI-2 and NBI-3) is higher than that of the specimen without it (NBI-1) by 90% and 97%, respectively.

At spans of 3.4 and 4.8 m, thin-slab specimens with end anchorages exhibit similar flexural failures, though they experience certain degrees of slip at the steel sheet–concrete interface at the anchoring end. This is mainly because the small-depth specimens have a low cross-sectional bending bearing capacity and low longitudinal shear stress at the steel sheet–concrete interface. Fig. 17 shows the load versus deflection curves and load versus slip curves of the specimens at failure.

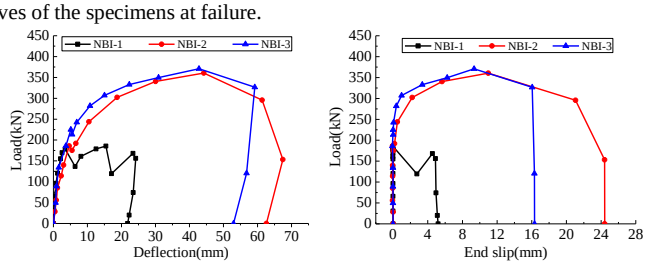

（a）Load – mid-span deflection curves （b）Load - end slip curves

Fig. 16 Load–deflection and Load–slip curves of the specimens with a span of 2.0 m

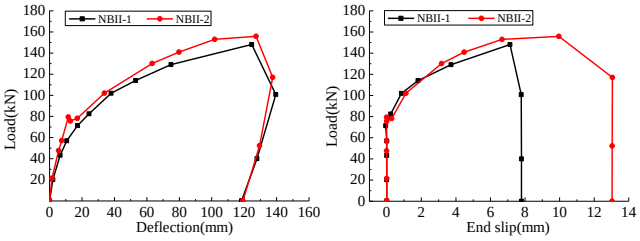

（a）Load – mid-span deflection curves （b）Load - end slip curves

Fig. 17 Load–deflection and Load–slip curves of the specimens with a span of 3.4 m

4.2.2. Long-span specimens

Fig. 18 shows the load–deflection curves and load–slip curves of the specimens with a span of 4.8 m. It reveals that the specimens of thin slabs experience similar stresses during the initial stage of loading. As the load increases, the specimen without end anchorage (NBⅢ-4) experiences end slip firstly. It also undergoes local failure of the bond at the steel sheet – concrete interface. As the stress at the interface redistributes, the slip is restrained, and the cross-sectional bearing capacity recovers at a certain degree. When the external load exceeds the bond at the profiled steel sheet–concrete interface, the specimen experiences a ductile longitudinal shear failure. The specimens with an end anchorage exhibit different behavior, mainly in that they experience significantly bigger slipping loads than the specimens without an end anchorage and exhibited flexural failure. The ultimate load of specimen NBⅢ-3 (with an end anchorage) is 56% higher than that of specimen NBⅢ-4 (without an end anchorage).

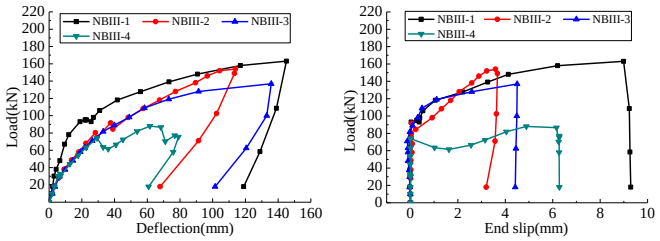

（a）Load – mid-span deflection curves （b）Load - end slip curves

Fig. 18 Load–deflection and Load–slip curves of the specimens with a span of 4.8 m

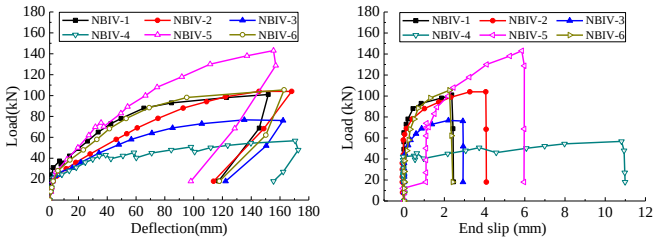

（a）Load – mid-span deflection curves （b）Load - end slip curves

Fig. 19 Load–deflection and Load–slip curves of the specimens with a span of 6.0 m

Fig. 19 presents the load–deflection curves and load–slip curves of the specimens with a span of 6.0 m. It shows that the specimens of thin slabs with spans of 6.0 m and 4.8 m exhibit similar failure behavior, except the end-anchored specimens with a span of 6.0 m, which experienced ductile longitudinal shear failure. In comparison, the specimens with a span of 4.8 m experienced flexural failure. At a span of 6.0 m, the bearing capacity of the specimen with an end anchorage (NBIV-3) is 36.8% higher than that of the specimen without it (NBIV-4). The additional reinforcement contributed to an improved cross-sectional bearing capacity but had a little effect on the stiffness of the specimen. They served to restrain the end slip; however, at high loads, the end slip increased with an increase in the flexural deformation, with the magnitude of slip depending on the strength of the end anchorage.

Fig. 18 and fig. 19 show that the bearing capacity of the composite slabs can be improved by increasing their cross-sectional depth or decking them with thick steel sheets. Increasing the cross-sectional depth can significantly improve the initial cross-sectional rigidity but has an insignificant effect on the cross-sectional rigidity and slip-resistance at high loads. In comparison, increasing the thickness of the profiled steel sheet can improve the interaction at the profiled steel sheet–concrete interface and, thereby, significantly reduce the slip at the steel sheet–concrete interface and cross-sectional rigidity at high loads.

Table 5 lists the characteristic loads, failure behavior, measured bearing capacity, and theoretical plastic bearing capacity of the dovetail-profiled specimens. It shows that the Mu/Mp ratio of the dovetail-profiled composite slabs can be effectively improved by strengthening their end anchorage, increasing the thickness of the profiled steel sheet, and implementing additional reinforcement at the troughs of the profiled steel sheet. This effectively improves the bond and longitudinal shear strength at the profiled steel sheet–concrete interface.

5. Parametric Analysis of Composite Slabs

To better reveal the failure behavior and performance of the composite slabs, specimens with different spans of 2.0, 3.4, and 6.0 m and a width of 1 m each were comparatively analyzed in terms of their load bearing capacity. The specimens in the same group had the same cross-sectional depth, span-depth ratio, and thickness of the steel sheet and were subjected to similar loading.

5.1. Short-span specimens

Fig. 20 shows the load–deflection curves and load–slip curves of without end-anchored specimens with a 2.0-m span. The small-span specimens without an end anchorage, OBI-3 and NBI-1, experience similar longitudinal shearfailure, except specimen OBI-3 (with a trapezoidal-profile), which experiences a brittle failure. Contrastingly, specimen NBI-1 (with a dovetail-profile) undergoes a ductile failure. The dovetail-profiled specimen performs much better than the trapezoidal-profiled specimen because the latter has a smaller end slip during the initial stage of loading, and the end slip has a direct impact on the bearing capacity of composite slabs. After the onset of the end slip, the dovetail-profiled composite slab specimens can recover their bearing capacity, whereas the trapezoidal-profile specimens experience a remarkable decrease in their bearing capacity. The load–deflection curves show that the dovetail-profiled specimens have slightly higher cross-sectional rigidities than the trapezoidal-profiled specimens, mainly owing to the different cross-sectional geometries.

Fig. 21 shows the load–deflection curves and load–slip curves of the end-anchored specimens with a 2.0-m span. It reveals that the specimens of

Table 5
Test result for load carrying capacity and failure mode of dovetail-profile specimens

No.	Specimens	P_{cr} （kN）	P_s （kN）	$P_{1/250}$ （kN）	P_u （kN）	M_u kN.m	M_p kN.m	M_u/M_p	$\triangle_u$ (mm)	s (mm)	Failure mode
1	NBⅠ-1	141	178.3	---	189	49.5	105.9	0.47	25.45	5.57	ductile
2	NBⅠ-2	155	185	243.6	360	92.2	105.9	0.87	65.96	12.62	ductile
3	NBⅠ-3	127	187.3	264.7	373	95.5	105.9	0.9	59.2	15.43	ductile
4	NBⅡ-1	50	71	71.4	149	83.4	83.7	1	137.1	7.79	flexural
5	NBⅡ-2	76	78	82.6	157	87.5	83.7	1.05	135.9	13.05	flexural
6	NBⅢ-1	50	90.1	96.1	163	127.3	120.6	1.06	142.9	9.23	flexural
7	NBⅢ-2	63	89.4	76	155	119.5	113.3	1.05	109.6	3.59	flexural
8	NBⅢ-3	48	70.2	76.6	137	106.5	91.1	1.17	116.0	2.59	flexural
9	NBⅢ-4	58	68.1	71.4	88	71.3	91.1	0.78	75.7	6.28	ductile
10	NBⅣ-1	35	73.1	60.3	100	102.4	157.5	0.65	151.8	2.37	ductile
11	NBⅣ-2	30	52.1	40.2	108	107.1	151.8	0.71	162.7	2.25	ductile
12	NBⅣ-3	28	49.7	42.8	78	80.1	120.6	0.66	161.6	2.92	ductile
13	NBⅣ-4	25.6	41.6	35.5	57	61.2	120.6	0.51	172.6	12.1	ductile
14	NBⅣ-5	38	82.1	66.5	152	146.7	186.0	0.79	154.6	1.11	ductile
15	NBⅣ-6	33	75.7	55.8	106	105.3	149.6	0.7	167.9	3.17	ductile

thick slab with the end anchorage have a remarkably high ductility. This is because the end-anchorage studs serve to restrain the slip at the profiled steel sheet–concrete interface, thereby indirectly improving the interaction at the steel sheet–concrete interface and significantly improving the bearing capacity. In addition, the maximum end slip is strongly correlated to the external load. Furthermore, from the onset of the interfacial slip to the ultimate bearing capacity, the end slip gradually increases with an increase in the external load, and the specimen exhibits good ductility.

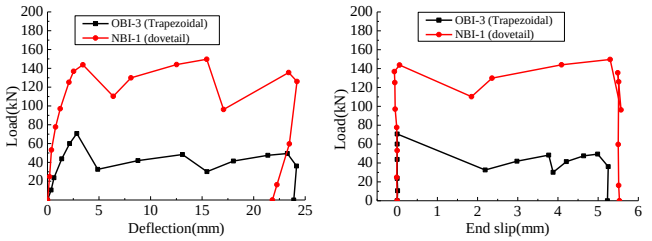

（a）Load – mid-span deflection curves （b）Load - end slip curves

Fig. 20 Load–deflection and Load–slip curves of 2.0 m span specimen without anchorage slabs

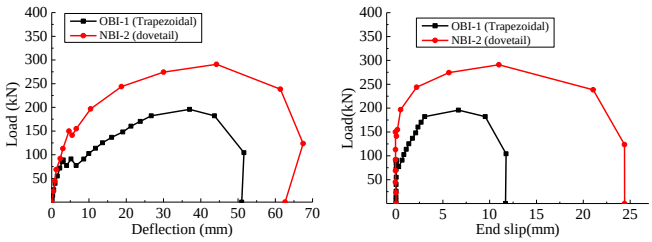

（a）Load – mid-span deflection curves （b）Load - end slip curves

Fig. 21 Load–deflection and Load–slip curves of 2.0 m span specimen with anchorage slabs

Fig. 21 shows the load–deflection curves and load–slip curves of the end-anchored specimens with a 2.0-m span. It reveals that the specimens of thick slab with the end anchorage have a remarkably high ductility. This is because the end-anchorage studs serve to restrain the slip at the profiled steel sheet–concrete interface, thereby indirectly improving the interaction at the steel sheet–concrete interface and significantly improving the bearing capacity. In addition, the maximum end slip is strongly correlated to the external load. Furthermore, from the onset of the interfacial slip to the ultimate bearing capacity, the end slip gradually increases with an increase in the external load, and the specimen exhibits good ductility.

Fig. 22 shows the load–deflection curves and load–slip curves of the specimens with a span of 3.4 m. These specimens have much larger span-depth ratios than the specimens with a span of 2.0 m. Fig. 22 also reveals that the mid-span deflections and end slips of the two kinds of composite slabs gradually increase with an increase in the external load and exhibit evident ductile behavior during the loading. The only difference is that the trapezoidal-profiled specimens undergo longitudinal shear failure, whereas the dove-tail specimens experience flexural failure.

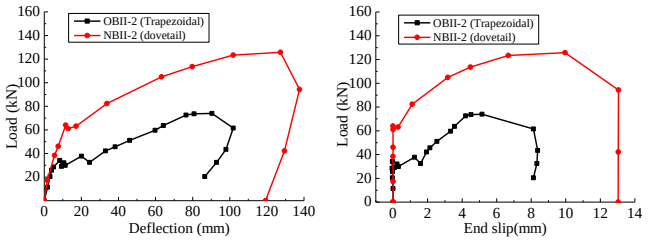

（a）Load – mid-span deflection curves （b）Load - end slip curves

Fig. 22 Load–deflection and Load–slip curves of 3.4 m span specimen with anchorage slabs

5.2. Long-span specimens

The long-span composite slab specimens with both the cross-sectional geometries were analyzed using the specimens with a span of 6.0 m. Fig. 23 shows the load–deflection curves and load–end slip curves of the specimens of thin slab without an end anchorage and with a 6.0 m span. It exhibits that the specimens with both the cross-sectional geometries experience ductile longitudinal shear failure. The dovetail-profiled specimens have a much better ductility than the trapezoidal-profiled specimens, and after the onset of the end slip, the former has a more evident increase in the bearing capacity than the latter. Furthermore, the end slip of the dovetail specimens changes with the variation in the load, whereas that of the trapezoidal-profiled specimens is accompanied by their failure.

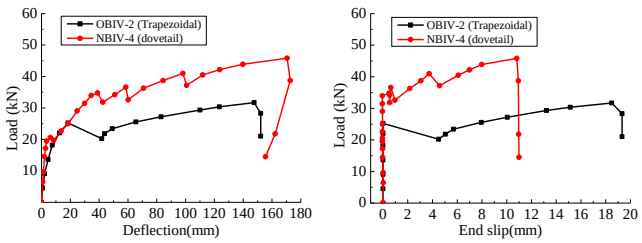

（a）Load – mid-span deflection curves （depth =200 mm） （b）Load - end slip curves （depth =200 mm）

Fig. 23 Load–deflection and Load–slip curves of 6.0 m span specimen without anchorage slabs

Fig. 24 shows the load–deflection curves and load–end slip curves of the end-anchored specimens of thin slab with a 6.0-m span. Fig. 24(a) shows that the trapezoidal-profiled specimens exhibit a more evident increase in the mid-span deflection and end slip during the loading than the dovetail-profiled specimens. The effect of the end anchorage on the bearing capacity improvement is less significant for the trapezoidal-profiled specimens than that for the dovetail-profiled specimens. The bearing capacity of the dovetail-profiled specimens is significantly improved, with the end slip restrained to a larger extent, whereas that of the trapezoidal-profile specimens improves only insignificantly. All the specimens with both the cross-sectional geometries undergo ductile failure, but the dovetail-profiled specimens have a significantly better ductility than he trapezoidal-profile specimens.

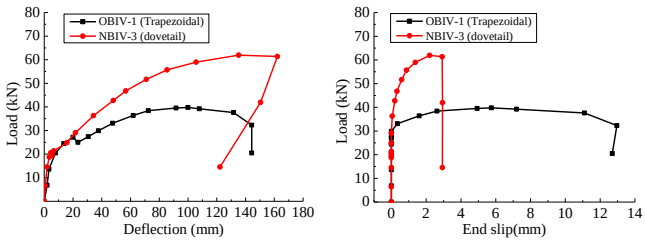

（a）Load – mid-span deflection curves (depth = 200mm) （b）Load - end slip curves (depth = 200mm)

Fig. 24 Load–deflection and Load–slip curves of 6.0 m span specimen with anchorage thin slabs

Fig. 25 shows the load–deflection curves and load–end slip curves of the end-anchored specimens of thick slab with a 6.0m span.

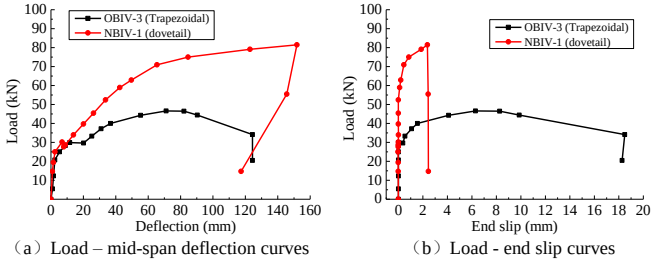

（a）Load – mid-span deflection curves (depth = 250mm) （b）Load - end slip curves (depth = 250mm)

Fig. 25 Load–deflection and Load–slip curves of 6.0 m span specimen with anchorage thick slabs

It shows that the end-anchorage studs contribute to a more significant improvement in the end slip and load bearing capacity of the dovetail-profiled specimens. In terms of the failure behavior, the end-anchorage studs contribute to only an insignificant improvement in the slip-resistance of the steel sheet–concrete interface of the trapezoidal-profiled specimens. All the

specimens with both the cross-sectional geometries experience ductile longitudinal shear failures, but the dovetail-profile specimens have a better ductility and slip-resistance. In comparison, the trapezoidal-profile specimens have an evident insufficient slip-resistance and a less safety buffer than the dovetail-profiled specimens.

Table 6 compares the measured load bearing capacity, M_u, and cross-sectional plastic bearing capacity, M_p, of the specimens with both the cross-sectional geometries. The composite slab specimens with an end anchorage have much larger M_u/M_p ratios than the specimens without it. It indicates that the end anchorage contributes to a significant improvement in the bond at the steel-sheet–concrete interface. At long spans, the specimens both with and without an end anchorage have similar M_u/M_p ratios. It indicates that the profiled steel sheet–concrete interface increases in area, and is more capable of restraining the slip at the interface at long spans, thereby indirectly improving the bond at the profiled steel-sheet–concrete interface.

Table 6
Comparison of bearing capacity between the trapezoidal-profile and dovetail-profile specimens

Span (m)	Depth (mm)	Anchorage	Trapezoidal profile				Dovetail profile			
			P_u	M_u	M_p	M_u/M_p	P_u	M_u	M_p	M_u/M_p
2.0	180	No	70.7	19.2	60.0	0.32	152.4	37.0	85.4	0.43
2.0	180	Yes	161.9	41.9	60.0	0.7	290.3	74.4	85.4	0.87
2.0	180	Yes	195.2	50.3	60.0	0.84	300.8	77.0	85.4	0.9
3.4	150	Yes	64.1	36.0	45.9	0.78	126.6	67.3	67.5	1
3.4	150	Yes	63.75	36.0	45.9	0.78	131.5	70.6	67.5	1.05
6.0	200	No	30.5	41.7	69.4	0.6	46.0	49.4	97．3	0.51
6.0	200	Yes	40.0	50.3	69.4	0.72	62.9	64.6	97.3	0.66
6.0	250	Yes	46.6	60.9	93.1	0.65	80.6	82.6	127.0	0.65

6. Conclusions

In this paper, the load bearing capacity and failure modes of composite slabs with different means of end anchorage were investigated through the test of 26 composite slab specimens with two cross-sectional profiles considering different details of the end anchorage. The effects of the parameters such as the end anchorage, span-to-depth ratio, and steel sheeting profile on the load bearing capacity and failure mode of the composite slabs both with and without an end anchorage were experimentally studied. The following conclusions can be drawn from this paper:

1. The end anchorage contributes to a significant improvement in the load bearing capacity and failure mode of the composite slabs. The contribution of the end anchorage to the bearing capacity improvement decreases with an increase in the span of composite slabs. Moreover, the degree of bearing capacity improvement varies with the cross-sectional geometry of the composite slabs.

2. Composite slabs without an end anchorage and subjected to external loading experience longitudinal shear failure in most cases, and the failure behavior of the composite slabs with the different cross-sectional geometries are related to the span-depth ratio. The composite slabs with an end anchorage subjected to external loading may experience ductile longitudinal shear failure or flexural failure.

3. The bearing capacity and slip-resistance of the composite slabs can be increased with the increasing of the profiled steel sheet. Additional reinforcement at the troughs of the profiled steel sheet can improve the load bearing capacity of the composite slabs but can only slightly improve their rigidity and slip-resistance.

4. Under the same conditions, the dovetail-profiled long-span composite slabs exhibit a better performance than the trapezoidal-profiled composite slabs.

Acknowledgements

This project was supported by the National Key R & D Program of China (2017YFC0703805), Key Research and Development Program of Liaoning Province (2017229006).

References

[1] Porter, M.L. and Greimann, L.F., “Shear-bond strength of studded steel deck slabs”, Proceedings of Sevenths International Specialty Conference on Cold-Formed Steel Structures, St. Louis, MO, USA., University of Missouri at Rolla, 285–306, 1984.
[2] Schuster, R. M. and Ling, W. C., “Mechanical Interlocking Capacity of Composite Slabs”, 5th International Specialty Conference on Cold-Formed Steel Structures, St. Louis, USA., 387-407, 1980.
[3] European Standard, “Eurocode 4:design of composite steel and concrete structures – part1-1: general rules and rules for buildings”, (EN 1994-1-1:2004), European Committee for Standardization, Brussels, 2004.
[4] Abdullah, R. and Samuel, E. W., “New modeling and evaluation procedures for horizontal shear bond in composite slabs”, Journal of Constructional Steel Research, 65(4), 891–899, 2009.
[5] Chen S., Shi X. and Qiu Z., “Shear bond failure in composite slabs-detailed experimental studies”, Journal of Steel and Composite Structures, 11(3), 233–250, 2011.
[6] Abdullah R., Kueh A.B.H., Izni S.I. and Samuel E.W., “Characterization of shear bond stress for design of composite slabs using an improved partial shear connection method”, Journal of Civil Engineering and Management, 21(6), 720-732, 2015.
[7] Valivonis J., “Analysis of behaviour of contact between the profiled steel sheeting and the concrete”, Journal of Civil Engineering And Management, 7(3), 187–194, 2006.
[8] Tsalkatidis T. and Avdelas A., “The unilateral contact problem in composite slabs: experimental study and numerical treatment”, Journal of Steel Construction, 66(3), 480-486, 2010.
[9] Chen S., Shi X. and Zhou Y., “Strength of composite slabs with end-anchorage studs”, Proceedings of the Institution of Civil Engineers-Structures and Buildings, 168(2), 127-140, 2014.
[10] Daniels B.J. and Crisinel M., “Composite slab behavior and strength analysis. Part I: calculation procedure”, Journal of Structural Engineering, ASCE, 119(1), 16–35, 1993.
[11] Rana M.M., Uy B. and Mirza O., “Experimental and numerical study of end anchorage in composite slabs”, Journal of Constructional Steel Research, 115, 372-386, 2015.
[12] Degtyarev V.V., “Strength of composite slabs with end anchorages. Part II: Parametric studies”, Journal of Constructional Steel Research, 94, 163-175, 2014.
[13] Patrick M. “Long-spanning composite members with steel decking”, Proc. Tenth Inter. Specialty Conf. on Cold-Formed Steel Structures, St. Louis, MO, USA, 81-102, 1990.
[14] Widjaja B.R., and Samuel E.W., “Developments in long span composite slabs”, Engineering Journal (New York), 37(2), 73-82, 2000.
[15] Jolly C.K. and Lawson R.M., “End anchorage in composite slabs: an increased load carrying capacity”, Journal of The Structural Engineer, 70(11), 202–205, 1992.
[16] Chen S., “Load carrying capacity of composite slabs with various end constraints”, Journal of Constructional Steel Research, 59(3), 385–403, 2003.
[17] Bode H. and Minas F., “Composite Slabs With and Without End Anchorage Under Static And Dynamic Loading”, Composite construction-conventional and innovative. International conference, 265-270, 1997.
[18] Gholamhoseini A., Gilbert R.I., Bradford M.A. and Chang Z.T., “Longitudinal shear stress and bond–slip relationships in composite concrete slabs”, Journal of Engineering structures, 69, 37-48, 2014.
[19] Johnson R.P. and Shepherd A.J., “Resistance to longitudinal shear of composite slabs with longitudinal reinforcement”, Journal of Constructional Steel Research, 82, 190-194, 2013.
[20] British Standard, Structural Use of Steelwork in Building-Part 4: Code of Practice for Design of Composite Slabs with Profiled Steel Sheeting, (BS-5950:1994), British Standard Institution, London, 1994.
[21] Ríos J.D., Cifuentes H., Martínez-De L.C.A. and Medina-Reguera F., “Numerical modelling of the shear-bond behaviour of composite slabs in four and six-point bending tests”, Journal of Engineering Structures, 133, 91-104, 2017.
[22] Abdullah R. and Samuel E.W., “Determination of composite slab strength using a new elemental test method”, Journal of Structural Engineering, 133(9), 1268–1277, 2007.
[23] Brekelmans J.W.P.M., Daniels B.J., Van Hove D.B.W.E.M. and Koukkari H., “Design Recommendations for Long Span Composite Slabs with Deep Profiled Steel Sheets”, Proceedings of the 1996 Engineering Foundation Conference on Composite Construction in Steel and Concrete III, Irsee, Germany. Workshop Composite Slabs, ASCE, 660-671, 1997.
[24] Johnson, R. P., “Composite Structures of Steel and Concrete: Beams, Slabs, Columns, and Frames for Buildings”, Third Edition, Blackwell Scientific, London 2008.